

Global and Local Alignment Networks for Unpaired Image-to-Image Translation

Guanglei Yang^{1,2} Hao Tang³ Humphrey Shi^{4,5,6} Mingli Ding¹
 Nicu Sebe² Radu Timofte³ Luc Van Gool³ Elisa Ricci^{2,7}

¹Harbin Institute of Technology ²DISI, University of Trento ³Computer Vision Lab, ETH Zurich
⁴University of Oregon ⁵UIUC ⁶Picsart AI Research (PAIR) ⁷Fondazione Bruno Kessler

Abstract

The goal of unpaired image-to-image translation is to produce an output image reflecting the target domain’s style while keeping unrelated contents of the input source image unchanged. However, due to the lack of attention to the content change in existing methods, the semantic information from source images suffers from degradation during translation. In the paper, to address this issue, we introduce a novel approach, Global and Local Alignment Networks (GLA-Net). The global alignment network aims to transfer the input image from the source domain to the target domain. To effectively do so, we learn the parameters (mean and standard deviation) of multivariate Gaussian distributions as style features by using an MLP-Mixer based style encoder. To transfer the style more accurately, we employ an adaptive instance normalization layer in the encoder, with the parameters of the target multivariate Gaussian distribution as input. We also adopt regularization and likelihood losses to further reduce the domain gap and produce high-quality outputs. Additionally, we introduce a local alignment network, which employs a pre-trained self-supervised model to produce an attention map via a novel local alignment loss, ensuring that the translation network focuses on relevant pixels. Extensive experiments conducted on five public datasets demonstrate that our method effectively generates sharper and more realistic images than existing approaches. Our code is available at <https://github.com/ygjwd12345/GLANet>.

1. Introduction

Recently, Generative Adversarial Networks (GANs) [16] have enabled the construction of powerful deep networks for domain adaptation [9, 40] and image-to-image translation [10, 15, 20, 25]. Focusing on image-to-image translation, most methods assume paired images among domains. However, for many tasks, pairwise information is hard to get and often not available. To tackle this problem, several works (*i.e.*, CycleGAN [59], DiscoGAN [26], Dual-

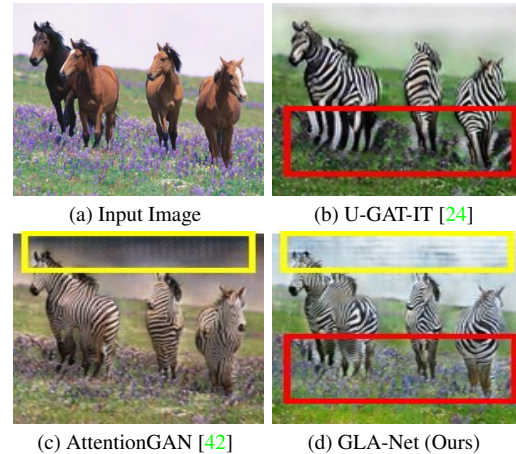


Figure 1. Comparison with state-of-the-art unsupervised image translation methods (*i.e.*, AttentionGAN [42] and U-GAT-IT [24]) on an example of Horse→Zebra task. The difference between the proposed GLA-Net and AttentionGAN [42] is marked with a yellow box while the difference between GLA-Net and U-GAT-IT [24] is marked with a red box. Better seen with magnification.

GAN [52], and StarGAN [7]) proposed to employ a cycle consistency loss in order to transfer images from the source to the target domain without pairwise supervision. While effective, these approaches suffer from performance degradation when significant changes must be operated to transfer an image to the other domain. Indeed, most existing methods can successfully transfer low-level information, such as color or texture, but struggle to control information changes at the semantic level.

To solve this problem, ContrastGAN [32] proposed a novel mask-conditional adversarial contrasting loss to enforce the produced output images to be semantically closer to the real data within the target category. However, this method requires object mask annotations in the training phase, thus implying a time-consuming labeling process. Similarly, Attention-GAN [6] introduced an extra attention network to produce a spatial attention map to distinguish among regions of interest and background and facilitate image generation. Following [6], Tang *et al.* [42] proposed to integrate the attention network into the generator to iden-

tify foreground objects and only modify them while keeping the background unchanged. U-GAT-IT [24] introduced adaptive layer-instance normalization to guide the attention-based models. However, the main problem with all these methods is that style and content change are not considered simultaneously. In other words, while these approaches either apply attention maps or instance normalization to control the transfer of semantics and style, they often fail to take care of both, the main reason being that style and content cannot be regarded as independent factors. An example of this phenomenon is illustrated in Figure 1. While U-GAT-IT [24] successfully manages to replace the horse style with the zebra style, there is still content degradation in the area of the image near the horse (red box in Figure 1 (b)). Differently, in AttentionGAN [42], while the attention map correctly forces the network to focus on the important areas of the image, some artifacts are visible in the style transition part (yellow box in Figure 1 (c)).

In this paper, we advance the state-of-the-art in unpaired image-to-image translation by proposing a novel framework, Global and Local Alignment Networks (*i.e.*, GLA-Net), which seamlessly addresses the subtasks of style transfer and semantic change (see Figure 2). Specifically, in the global alignment network, we use the style features predicted by our network to replace the learnable scale and shift parameter in instance normalization, thus implementing a novel and more effective style transform. Moreover, we introduce a global alignment loss to enforce similarities among the two multivariate Gaussian distributions obtained from the source and target domains. Since the global alignment network is designed to account for style transfer, the semantic information of unrelated pixels or backgrounds suffers from degradation during image translation in the case of significant changes. To support the global alignment network, we further propose a novel local alignment network. It helps the generator to focus on essential pixels during image translation and reduce the content degradation in irrelevant image parts as much as possible. Thanks to the combination between the global and the local alignment network, the generator is able to successfully operate a global style transfer and produce consistent content changes.

The contributions of this paper are summarized as follows:

- We propose a novel framework for unpaired image-to-image translation which simultaneously addresses style transfer and semantic content change tasks within the same deep model, thus enabling higher accuracy and flexibility in style and content modification.
- We introduce GLA-Net, a novel deep architecture with two main components: a global and a local alignment network. The global alignment network enables accurate style transfer, thanks to an MLP-Mixer style encoder and a feature alignment strategy. The local alignment network

integrates a self-supervised attention map to mitigate the content degradation problem of existing methods.

- Extensive experiments conducted on five publicly available datasets demonstrate that GLA-Net can generate photo-realistic images with higher quality and sharper details than existing methods.

2. Related Work

Image-to-image translation methods [30, 33, 43, 46, 59] operate by transferring the style of images from a source to a target domain while preserving the content information. Earlier methods [4, 22, 38, 46] mainly focused on paired image-to-image translation, thus heavily relying on a reconstruction loss computed on paired images among domains. However, in many real-world applications, pairwise information is not available. To address this issue, several works considered a cycle consistency loss in order to preserve the consistency at image level [26, 52, 59] or at feature level [21, 60]. However, as the cycle consistency loss treats all pixels equally, these models struggle to focus on the essential parts of the images. To solve this problem, attention maps can be integrated to guide the translation model similar to other computer vision tasks such as depth estimation [49, 51] and semantic segmentation [14, 19]. Two strategies are possible to create attention modules that compute the region of interest for the image translation task. The first strategy consists in using extra data to provide attention. For instance, ContrastGAN [32] used object mask annotations as extra input data. InstaGAN [35] also proposed to incorporate the object segmentation mask to improve multi-instance transfiguration. The second strategy is to train another segmentation or attention model to generate attention maps and insert them into the system. This strategy was considered in [50], SPADE [38], SEAN [61] and AttentionGAN [42].

Another problem with earlier approaches for unsupervised image-to-image translation [26, 59] is that, only with cycle consistency loss, the local semantic information tends to be destroyed in image-to-image translation, thus affecting the overall quality of the generated image. To address this issue, Park *et al.* [37] proposed CUT and applied contrastive learning to learn the correspondence between associated patches. Similarly, FSeSim [57] introduced a spatially-correlative loss to capture patch-wise spatial relationships within an image. In this paper, we introduce a different strategy to address this problem and propose a novel local alignment network that integrates a self-attention mechanism.

Ensuring effective style transfer is a fundamental problem in image-to-image translation. Style transfer models typically operate by normalizing feature tensors with instance-specific mean and standard deviation, *i.e.*, adopt Instance Normalization (IN) [12, 45]. Adaptive Instance

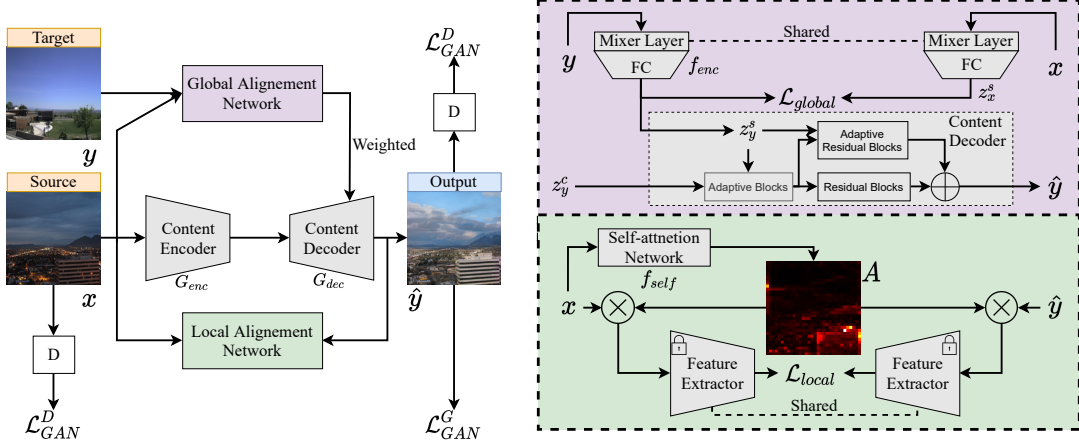


Figure 2. Overview of GLA-Net. The whole architecture is composed by a global alignment network, a local alignment network, a content encoder G_{enc} , and a content decoder G_{dec} . In the global alignment network, we employ a style encoder f_{enc} with different fully-connected layers but shared-weight MLP-Mixer layers to extract style features, z_x^s and z_y^s , from source image x and target image y . The global alignment loss \mathcal{L}_{global} aims to make style feature between the two domain as close as possible. The style features of the target image z_y^s , including μ_y, σ_y , are also used to assign weights and biases to the adaptive blocks of the content decoder. As for the local alignment network, we adopt a self-attention network f_{self} to get an attention map A which weights source image and output image, and then is fed to the local alignment loss \mathcal{L}_{local} . In this way, it can help the network to avoid content destruction in irrelevant part. The symbol \otimes and \oplus denotes element-wise multiplication and element-wise addition, respectively.

Normalization (AdaIN) [20] represent an improvement over traditional IN. In image-to-image translation, to ensure better style transfer among domains, U-GAT-IT [24] proposes an adaptive layer-instance normalization, whose parameters are learned from datasets during the training stage. Different from U-GAT-IT [24], in this paper, we propose a distribution alignment approach to extend AdaIN and integrate it into our global alignment network. Furthermore, while all the above methods focus on specific aspects related either to style transfer or semantic content modification, in this paper, we propose for the first time an architecture that simultaneously handles the style and content changes in a holistic manner.

3. Global and Local Alignment Networks

In this paper, we present a novel framework, *i.e.*, Global and Local Alignment Networks (GLA-Net), to simultaneously realize style transfer and semantic content modification for unpaired image-to-image translation. In the following, we first introduce the whole framework architecture in Section 3.1. Then, in Section 3.2 and Section 3.3, we introduce the details of our GLA-Net. Finally, we discuss the loss functions used in our framework in Section 3.4.

3.1. Framework Overview

Given a collection of images $\mathcal{X} \subset \mathbb{R}^{H \times W \times C}$ from a source domain, our main goal is to learn a model G that receives the image $x \in \mathcal{X}$ as input and transfers it into the target domain $\mathcal{Y} \subset \mathbb{R}^{H \times W \times C}$, in a way to jointly convert the style and semantic content together.

Figure 2 gives an overview of the proposed framework.

Besides a content encoder G_{enc} and a content decoder G_{dec} , the proposed method also contains two modules, *i.e.*, a global alignment network and a local alignment network. The purpose of the global alignment network is to replace the source domain style with the target domain style, while the local alignment network is designed to ensure that the translation network focuses on relevant pixels in the image. The content encoder G_{enc} and the content decoder G_{dec} of the generator G are applied sequentially to generate an output image, *i.e.*, $\hat{y} = G_{dec}(z_x^c) = G_{dec}(G_{enc}(x))$. The global alignment network employs a style encoder f_{enc} including shared MLP-Mixer layers [44] but different fully-connected layers. It extracts style features from source image x and target image y . The outputs of the style encoder are denoted as z_x^s and z_y^s , respectively. In detail, z_x^s includes an N -dimensional vector of multivariate Gaussian parameters (μ_x, σ_x) , which represent the style features of the source image x . The relationship between the Gaussian parameters μ_x, σ_x and z_x^s is defined as follow:

$$\mu_x = z_x^s[1 : N], \quad \sigma_x = z_x^s[N + 1 : 2N], \quad (1)$$

Similarly, z_y^s comprises μ_y and σ_y . The global alignment loss \mathcal{L}_{global} aims to make the style features between the two domains as close as possible. The style features of the target image, μ_y, σ_y , are also used to provide weights to the IN layer of the content decoder. The local alignment network integrates a self-attention network f_{self} which provides an attention map A . The source image x and the output image \hat{y} , weighted by the attention map A respectively, are provided to the feature extractor f_{ext} supervised by a local alignment loss \mathcal{L}_{local} .

3.2. Global Alignment Network

MLP-Mixer-Based Style Encoder. Extracting style features plays a vital role in image-to-image translation, which is particularly important in our global alignment network. Different from previous works which use multiple Res-Blocks [24, 39] as style encoder, we proposed to employ MLP-Mixer layer [44], which is an effective but conceptually and technically simple alternative, with fully-connected layers (the related experiments in supplementary material further confirms this augment). Following [11, 44], we divide the input image into a sequence of flattened 2D paths, $x_p \in \mathbb{R}^{n \times (P^2 \cdot C)}$, and compute per-patch linear embeddings. Then the output of per-patch linear embedding is passed through Mixer layers and fully-connected layers to get the final style feature. Given the input image $x \in \mathbb{R}^{H \times W \times C}$, the full style encoder process is defined as follow:

$$z = [x_{class}; x_p^1 E; x_p^2 E; \dots; x_p^n E] + E_{pos}, \quad (2)$$

$$z' = z + W_2 \phi(W_1 LN(x)), \quad (3)$$

$$Z'' = z' + W_4 \phi(W_3 LN(x)), \quad (4)$$

$$Z^s = FC(Z''), \quad (5)$$

where ϕ is an element-wise nonlinearity [17], LN indicates layer normalization and $W_{1,2,3,4}$ are the weights of the convolution layers. Eq. (3) and Eq. (4) construct a basic MLP-Mixer layer. We denote the number of MLP-Mixer layers as depth.

Improved Adaptive Instance Normalization. Inspired by instance normalization (IN) [45], we adopt an adaptive instance normalization layer in the content encoder to transfer the source style to the target style. The original IN is formulated as:

$$IN(x) = \gamma \frac{x - \mu(x)}{\sigma(x)} + \kappa, \quad (6)$$

where $\sigma(\cdot)$, $\mu(\cdot)$ denote standard deviation and mean computed via the spatial dimension within each channel of the input and γ, κ are learnable scale and shift parameters. According to [24], this method is more suitable for style transfer tasks while failing in image translation tasks that require significant content changes. Recent works [20, 24, 58] proposed to fuse the mean and standard deviation of both domains to address this issue. For example, AdaIN [20] replaces γ, κ in Eq. (6) with the mean and standard deviation of the target image,

$$AdaIN(x) = \sigma(y) \frac{x - \mu(x)}{\sigma(x)} + \mu(y), \quad (7)$$

In this work, different from the above methods, we replace the learnable scale and shift parameters in Eq. (6) with style features predicted by a style encoder. To sufficiently represent the style features, we compute predictions of N

sets $(\mu_y^i, \sigma_y^i)_{i \in 1 \dots N}$. Thus, the formula of adaptive instance normalization is updated as:

$$AdaIN^{new}(x) = \sigma_y \frac{x - \mu(x)}{\sigma(x)} + \mu_y, \quad (8)$$

Style Feature Alignment. Having multivariate Gaussian distributions, $\mathcal{N}(\mu_x, \sigma_x^2)$ and $\mathcal{N}(\mu_y, \sigma_y^2)$, from the source domain and the target domain according to Eq. (1), we adapt a likelihood loss \mathcal{L}_l from [56] to force the two multivariate Gaussian distributions to be close to each other. The likelihood loss is defined as:

$$\mathcal{L}_l = -\frac{1}{2\sigma_x^2} \sum_{i=1}^N (s_y^i - \mu_x)^2, \quad (9)$$

where s_y are N sample from multivariate Gaussian distribution $\mathcal{N}(\mu_y, \sigma_y^2)$. The number of samples is equal to the dimensions of predicted Gaussian distributions in any domain. We also employ a regularization loss \mathcal{L}_r to encourage the model to predict various Gaussian distributions and to learn meaningful latent representations according to InfoVAE [56]. The regularization loss \mathcal{L}_r is calculated by:

$$\mathcal{L}_r = -D_{KL}(\mathcal{N}(0, 1), \mathcal{N}(\mu_x, \sigma_x^2)), \quad (10)$$

where D_{KL} represents Kullback–Leibler divergence and $\mathcal{N}(0, 1)$ represents a unit Gaussian. Therefore, the whole global alignment loss is as follows:

$$\mathcal{L}_{global} = \lambda_l \mathcal{L}_l + \lambda_r \mathcal{L}_r, \quad (11)$$

where both λ_l and λ_r are set to 1 following [56].

3.3. Local Alignment Network

The global alignment network ensures accurate style transfer. However, for image-to-image translation tasks with significant content changes, the network will easily focus on unimportant pixels, as discussed in Section 4.4. To address this problem, we propose a novel local alignment network supervised by a pixel-wise spatial-correlative loss. We consider DeiT-S-p8 [3] as our self-attention network f_{self} and compute the attention map A as $A = f_{self}(x)$ and subsequently a spatially-correlative map [57],

$$S_x = f_{ext}(A \cdot x)^T f_{ext}(A \cdot x)_*, \quad (12)$$

where $(\cdot)_*$ indicates corresponding features of image x in a path of points. In the same way, replacing x with \hat{y} in the above equation, we can get the spatially-correlative map of generated image $S_{\hat{y}}$. Additionally, we define the pixel-wise spatial-correlative loss as follow:

$$\mathcal{L}_{local} = \|1 - \cos(S_x, S_{\hat{y}})\|, \quad (13)$$

This loss helps the generator to avoid content destruction in the irrelevant image part. In fact, it evaluates every pixel importance by the spatially-correlative map and supports the spatial similarity to be consistent at all points.

3.4. Overall Optimization Objective

Our framework also integrates a discriminator, as shown in Figure 2. Hence, besides the global alignment loss and local alignment loss, our framework also employs a generative adversarial loss. This adversarial loss $\mathcal{L}_{GAN} = \mathcal{L}_{GAN}^D + \mathcal{L}_{GAN}^G$ can be formulated as follows,

$$\mathcal{L}_{GAN}^D = -\mathbb{E}[\log D(y)] - \mathbb{E}[\log(1 - D(\hat{y}))], \quad (14)$$

$$\mathcal{L}_{GAN}^G = \mathbb{E}[\log(1 - D(\hat{y}))], \quad (15)$$

The whole optimization objective of the proposed GLA-Net can be expressed as:

$$\mathcal{L} = \mathcal{L}_{GAN} + \lambda_{global}\mathcal{L}_{global} + \lambda_{local}\mathcal{L}_{local}, \quad (16)$$

where λ_{global} and λ_{local} are hyper-parameters are controlling the importance of the corresponding loss term, which are empirically set to 1 and 10 in all our experiments, respectively. The detailed parameter selection process is discussed in the supplementary material.

4. Experiments

4.1. Experiment Setups

Datasets. We tested our method on various image-to-image translation tasks, including single-modal (Cityscapes [8], Cat→Dog [7], Horse→Zebra [59]) and multi-modal translation (Winter→Summer [59], Night→Day [22]) problems. The Cityscapes dataset contains thousands of finely annotated images taken in street scenes with pixel-level annotations. Cat→Dog contains 5,000 training and 500 validation images from AFHQ dataset [7]. The Horse→Zebra dataset consists of about 2,500 images of horse and zebra in different scenes. Winter→Summer [59] is downloaded using Flickr API with the tag “yosemite” and the “datetaken” field, including 1,273 summer images and 854 winter images. Night→Day, trained on [28], includes 17,823 training images extracted from 91 webcams. For all the datasets, we resize the images to the same resolution of 256×256 pixels.

Implementation Details. We choose FSeSim [57] as the baseline architecture and replace the spatially-correlative loss with our local alignment loss. Specifically, we use the UNet-based content encoder and decoder with AdaIN [23] in the global alignment network. We also adopt MLP-Mixer with depth 1 as our style encoder in the global alignment network. The ImageNet-pretrained VGG16 [41] is chosen as our feature extractor, where we use feature from layers conv2d_{4,7,9}. For all the experiments, we use the Adam solver [27] with a batch size of 1. All networks were trained from scratch with a learning rate of 1×10^{-4} . The dimension of the predicted multivariate Gaussian distribution N is set to 32 for all experiments. The training lasts 400 epochs in total. We apply PyTorch to implement our

framework, and we perform all experiments on an NVIDIA Titan XP GPU.

Evaluation Protocols. Following the evaluation protocols from [18, 37, 57, 59], we choose a few metrics to assess the visual quality and measure the domain distance. For the first, we utilize the Fréchet Inception Distance (FID) [18], which empirically estimates the distribution of target and generated images in a deep network space and computes the divergence between them. In this paper, it is used for both single- and multi-modal image translation tasks. We also use Kernel Inception Distance (KID) [2], which is the squared maximum mean discrepancy between Inception representations, to compare with methods only reporting KID results. To evaluate the Cityscapes task, we feed the generated images to the pretrained semantic segmentation network DRN [53]. Then the outputs of DRN are used to compute the mean average precision (mAP), pixel-wise accuracy (pAcc), and average class accuracy (cAcc), as done in [22, 37, 38, 54]. Meanwhile, we also use the average LPIPS distance [55] to evaluate the multi-modal image translation, which measures the distance between two images in a feature domain and correlates well with human perception. Finally, we consider density and coverage (D&C) [36], which uses density and coverage to measure similarity between the generated manifold and the target manifold.

4.2. Single-Modal Unpaired Image Translation

We compare our method with state-of-the-art methods, *i.e.*, U-GAT-IT [24], CWT-GAN [29], IrwGAN [48], DistanceGAN [1], GcGAN [13], CUT [37], and FSeSim [57] on single-modal image translation. According to whether the methods are one-sided framework, Table 1 is divided into upper (double-sided framework) and lower (one-sided framework) parts for a fair comparison. We pick up three popular datasets on single-modal image translation, *i.e.*, cityscapes, cat→dog, and horse→zebra, all of which belong to the task requiring style transfer and large content changes. Unsurprisingly, we find the methods which solely focus on style transfer like U-GAT-IT [24] and the attention-based networks, such as AGGAN [34] and AttentionGAN [42], obtain unsatisfactory performance on these three tasks. In contrast, since our approach comprises both a style transform network and an attention-based network, it achieves the best results considering most of the metrics in Table 1. Moreover, comparing our method with other one-sided methods, *i.e.*, CUT [37] and FSeSim [57], our method significantly outperforms these methods.

Qualitative results with several challenging methods on single-modal image translation are shown in Figure 3. We find that the images generated by our method have higher quality and sharper details than those obtained with previous approaches. This confirms the fact that since our work



Figure 3. Qualitative results with the several challenging methods, *i.e.*, FSeSim [57], CUT [37], CycleGAN [59], MUNIT [21], DRIT [30], DistanceGAN [1], GcGAN [13], on three benchmark datasets of single-modal image translation.

Table 1. Quantitative comparison on single-modal image translation. * means results come from our re-implementation. KID means Kernel Inception Distance $\times 100$.

Method	One-Sided	Cityscapes				Cat \rightarrow Dog		Horse \rightarrow Zebra	
		mAP \uparrow	pAcc \uparrow	cAcc \uparrow	FID \downarrow	FID \downarrow	KID \downarrow	FID \downarrow	KID \downarrow
CycleGAN [59]	\times	20.4	55.9	25.4	76.3	85.9	6.93	77.2	3.24
MUNIT [21]	\times	16.9	56.5	22.5	91.4	104.4	2.42	133.8	6.92
DRIT [30]	\times	17.0	58.7	22.2	155.3	123.4	4.57	140.0	7.40
NICE-GAN [5]	\times	-	-	-	-	48.8	1.58	65.9	2.09
AttentionGAN [42]	\times	-	-	-	-	-	-	68.6	2.03
U-GAT-IT [24]	\times	-	-	-	-	-	7.07	-	7.06
CWT-GAN [29]	\times	-	-	-	-	46.3	-	85.4	-
IrwGAN [48]	\times	-	-	-	-	61.0	2.07	79.4	1.83
DistanceGAN [1]	\checkmark	8.4	42.2	12.6	81.8	155.3	-	72.0	-
AGGAN [34]	\checkmark	-	-	-	-	-	9.84	-	6.93
GcGAN [13]	\checkmark	21.2	63.2	26.6	105.2	96.6	-	86.7	-
CUT [37]	\checkmark	24.7	68.8	30.7	56.4	76.2	-	45.5	-
FSeSim [57]	\checkmark	-	69.4	-	53.6	78.9*	3.72*	40.4	-
GLA-Net (Ours)	\checkmark	23.5	76.2	31.8	51.8	66.6	2.94	37.7	0.87

seamlessly integrates two components, it ensures higher flexibility in style and content modification. Our network better focuses and changes the most important parts of the image while preserving the background information.

4.3. Multi-Modal Unpaired Image Translation

To verify the versatility of our algorithm, we also provide a comparison among our method and other state-of-the-art methods, *i.e.*, NICE-GAN [5], FSeSim [57] and CWT-GAN [29], on multi-modal unpaired image translation tasks. The chosen benchmarks include Winter \rightarrow Summer dataset and Night \rightarrow Day datasets, which are regarded as typical style transfer tasks. According to the results in Table 2, our method significantly surpasses FSeSim [57]. In detail, in terms of FID, there is an 18.6 and 43.5 improvement between our method and FSeSim on both datasets, respectively. Moreover, our method achieves better results than the recent SOTA, CWT-GAN [29] and NICE-GAN [5]. Qualitative results on multi-modal image translation are shown in Figure 4. What is more, in terms of D&C, our method reaches the new SOTA leaving a considerable margin with other methods in the Winter \rightarrow Summer

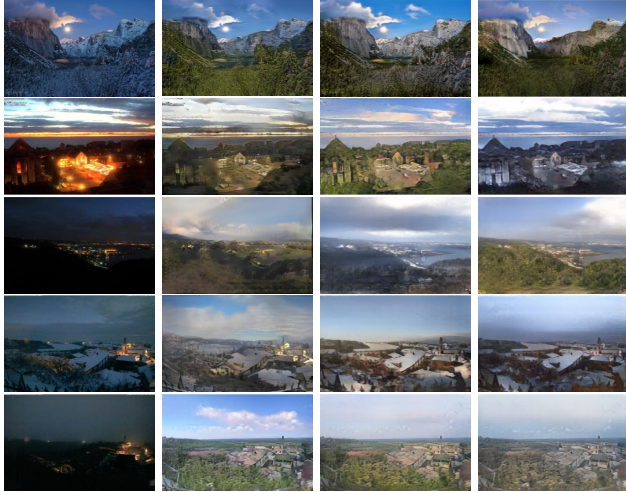
Table 2. Qualitative comparison on multi-modal image translation.

Method	Winter \rightarrow Summer		Night \rightarrow Day	
	FID \downarrow	D & C \uparrow	FID \downarrow	D & C \uparrow
BicycleGAN [47]	99.2	0.536 / 0.667	290.9	0.375 / 0.515
MUNIT [21]	97.4	0.439 / 0.707	267.1	0.271 / 0.548
DRIT++ [31]	93.1	0.494 / 0.753	258.5	0.298 / 0.631
FSeSim [57]	90.5	0.501 / 0.779	234.3	0.332 / 0.638
CWT-GAN [29]	77.0	-	-	-
NICE-GAN [5]	76.4	-	-	-
GLA-Net (Ours)	71.9	0.879 / 0.894	190.8	0.301 / 0.629

task while our method also gets an acceptable result. Similar to single-modal image translation, the results generated by our method are more photo-realistic than those obtained by previous methods.

4.4. Ablation Study

To demonstrate the effectiveness of different components of the proposed GLA-Net, we train several model variants and test them on both single- and multi-modal unpaired image translation tasks. The results are reported in Table 3. We choose FSeSim [57] as our baseline, and repro-

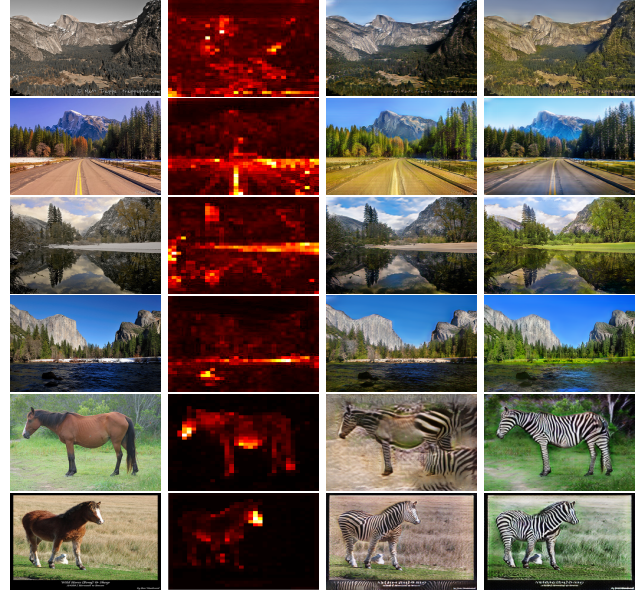


(a) Input (b) Ours (c) FSeSim [57] (d) MUNIT [21]
 Figure 4. Qualitative results on two datasets, *i.e.*, Winter→Summer and Day→Night, of multi-modal image translation.

duced results are reported in the first row of Table 3. According to results in Table 3, adding a global alignment network or a local alignment network significantly improves performance according to all metrics. It proves the effectiveness of both sub-networks.

We provide some visualization results of our attention maps in Figure 5. To demonstrate the impact of the attention, the input image, the output of the baseline method, and the output of baseline with the local alignment network are shown in Figure 5. The pixels whose color is closer to yellow are regarded as more important by the network. Conversely, darker pixels are considered less relevant. The figure clearly shows that when adding the attention map into the baseline model, the visual quality of important pixels gets significant improvements. It proves that the local alignment network effectively helps the generator pay more attention to important pixels during translation.

According to Table 3, when adding $AdaIN^{new}$ to the baseline, the style translation network works well for the style transfer tasks (*e.g.*, winter→summer) but is typically unsuccessful for shape change tasks (*e.g.*, horse→zebra). The visualisation results in Figure 7 (b) and (c) support this claim. Some of the semantic information belonging to the background pixel gets the completely wrong translation on the horse→zebra task. However, adding the global alignment loss into the style translation network clearly provides a benefit. The associated qualitative results are shown in Figure 7. From the figure, better image translations are observed. However, compared with (a) and (d) in Figure 7, there is still a little content degradation in the background. For example, the area between the two horses in the first image of Figure 7 and the area around the horse’s head in the second image are also striped.



(a) Input (b) Attention (c) Baseline (d) w/ \mathcal{L}_{local}
 Figure 5. Visualisation of generated attention maps on two benchmark datasets, *i.e.*, Winter→Summer and Horse → Zebra.

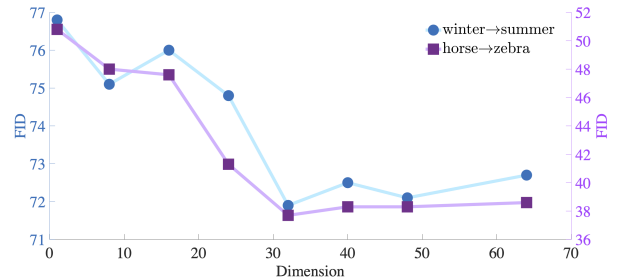


Figure 6. Ablation study of the dimensions of predicted multivariate Gaussian distribution.

To understand how the dimension of the predicted multivariate Gaussian distributions influences the global alignment network, we perform an ablation study of the predicted multivariate Gaussian distribution dimensions. We choose N sequence from [1, 8, 16, 24, 32, 40, 48, 64] and test it in both Winter→Summer and Horse→Zebra tasks. The results are shown in Figure 6. When the value is higher than 32, the performance of our method becomes stable. In this case, we set N as 32 for all our experiments.

4.5. Limitation

We show some failure results on single-modal image translation and multi-modal image translation in Figure 8 to discuss our method’s limitations. According to the Horse→Zebra task’s results, the self-attention network incorrectly provides attention when both of them coexist in the same picture. On the other hand, the failure results on the Winter→Summer task prove that when the object of interest occupies a large part of the image, the self-attention network cannot identify it correctly. In the future, we plan to investigate self-distillation [3] to solve these problems.



(a) Input Image (b) Baseline (c) w/ AdaIN (d) w/ Global Alig. (e) w/ Local Alig. (f) GLA-Net (Our Full)

Figure 7. Visualisation results of different methods in Table 3.

Table 3. Ablation study of our global and local alignment method on both single- and multi-modal unpaired image translation. $AdaIN^{new}$, \mathcal{L}_{global} and \mathcal{L}_{local} is defined by Eq. (8), (11), and (13), respectively.

Method	$AdaIN^{new}$	\mathcal{L}_{global}	\mathcal{L}_{local}	Horse \rightarrow Zebra			Winter \rightarrow Summe		
				LPIPS \downarrow	FID \downarrow	D & C \uparrow	LPIPS \downarrow	FID \downarrow	D & C \uparrow
Baseline				0.743	46.5	0.825/0.800	0.792	89.1	0.727/0.739
w/ AdaIN	✓			0.767	51.7	0.819/0.794	0.758	79.0	0.767/0.839
w/ Global Alignment	✓	✓		0.722	39.7	0.966/0.936	0.761	74.8	0.856/0.841
w/ Local Alignment			✓	0.732	40.6	0.953/0.924	0.755	78.4	0.869/0.846
GLA-Net (Our Full)	✓	✓	✓	0.714	37.7	0.977/0.946	0.750	71.9	0.879/0.894



(a) Input (b) Attention (c) Ours

Figure 8. Failure results on single-modal image translation and multi-modal image translation.

5. Conclusion

We proposed GLA-Net, a new approach for unpaired image-to-image translation which simultaneously addresses two subtasks, *i.e.*, style transfer and semantic content change. Each subtask is handled by the corresponding sub-network. Specifically, we proposed a global alignment network for style transfer, which integrates an MLP-Mixer style encoder and a feature alignment strategy based on a new adaptive instance normalization scheme. We also introduced a local alignment network for semantic content modification, which integrates a new self-attention mechanism. We compared our approach with several state-of-the-art methods, conducting experiments on five publicly available datasets, demonstrating the superiority of our proposed GLA-Net.

Broader Impacts. It is well-known that image and video generation methods based on GANs can be potentially used for malicious applications. However, focusing on the specific approach proposed here and on the application of image translation, we believe that the potential benefits, *e.g.*, in creative industry tasks outweigh the threats.

References

- [1] Sagie Benaim and Lior Wolf. One-sided unsupervised domain mapping. In *NeurIPS*, 2017. 5, 6
- [2] Mikołaj Bińkowski, Danica J Sutherland, Michael Arbel, and Arthur Gretton. Demystifying mmd gans. In *ICLR*, 2018. 5
- [3] Mathilde Caron, Hugo Touvron, Ishan Misra, Hervé Jégou, Julien Mairal, Piotr Bojanowski, and Armand Joulin. Emerging properties in self-supervised vision transformers. In *ICCV*, 2021. 4, 7
- [4] Qifeng Chen and Vladlen Koltun. Photographic image synthesis with cascaded refinement networks. In *ICCV*, 2017. 2
- [5] Runfa Chen, Wenbing Huang, Binghui Huang, Fuchun Sun, and Bin Fang. Reusing discriminators for encoding: Towards unsupervised image-to-image translation. In *CVPR*, 2020. 6
- [6] Xinyuan Chen, Chang Xu, Xiaokang Yang, and Dacheng Tao. Attention-gan for object transfiguration in wild images. In *ECCV*, 2018. 1
- [7] Yunjey Choi, Youngjung Uh, Jaejun Yoo, and Jung-Woo Ha. Stargan v2: Diverse image synthesis for multiple domains. In *CVPR*, 2020. 1, 5
- [8] Marius Cordts, Mohamed Omran, Sebastian Ramos, Timo Rehfeld, Markus Enzweiler, Rodrigo Benenson, Uwe Franke, Stefan Roth, and Bernt Schiele. The cityscapes dataset for semantic urban scene understanding. In *CVPR*, 2016. 5
- [9] Dengxin Dai and Luc Van Gool. Dark model adaptation: Semantic image segmentation from daytime to nighttime. In *ITSC*, 2018. 1
- [10] Chao Dong, Chen Change Loy, Kaiming He, and Xiaoou Tang. Image super-resolution using deep convolutional networks. *TPAMI*, 2015. 1
- [11] Alexey Dosovitskiy, Lucas Beyer, Alexander Kolesnikov, Dirk Weissenborn, Xiaohua Zhai, Thomas Unterthiner, Mostafa Dehghani, Matthias Minderer, Georg Heigold, Sylvain Gelly, et al. An image is worth 16x16 words: Transformers for image recognition at scale. In *ICLR*, 2021. 4
- [12] Vincent Dumoulin, Jonathon Shlens, and Manjunath Kudlur. A learned representation for artistic style. In *ICLR*, 2017. 2
- [13] Huan Fu, Mingming Gong, Chaohui Wang, Kayhan Batmanghelich, Kun Zhang, and Dacheng Tao. Geometry-consistent generative adversarial networks for one-sided unsupervised domain mapping. In *CVPR*, 2019. 5, 6
- [14] Jun Fu, Jing Liu, Haijie Tian, Yong Li, Yongjun Bao, Zhiwei Fang, and Hanqing Lu. Dual attention network for scene segmentation. In *CVPR*, 2019. 2
- [15] Leon A Gatys, Alexander S Ecker, and Matthias Bethge. Image style transfer using convolutional neural networks. In *CVPR*, 2016. 1
- [16] Ian Goodfellow, Jean Pouget-Abadie, Mehdi Mirza, Bing Xu, David Warde-Farley, Sherjil Ozair, Aaron Courville, and Yoshua Bengio. Generative adversarial nets. In *NeurIPS*, 2014. 1
- [17] Dan Hendrycks and Kevin Gimpel. Gaussian error linear units (gelus). *arXiv*, 2016. 4
- [18] Martin Heusel, Hubert Ramsauer, Thomas Unterthiner, Bernhard Nessler, and Sepp Hochreiter. Gans trained by a two time-scale update rule converge to a local nash equilibrium. In *NeurIPS*, 2017. 5
- [19] Jie Hu, Li Shen, and Gang Sun. Squeeze-and-excitation networks. In *CVPR*, 2018. 2
- [20] Xun Huang and Serge Belongie. Arbitrary style transfer in real-time with adaptive instance normalization. In *ICCV*, 2017. 1, 3, 4
- [21] Xun Huang, Ming-Yu Liu, Serge Belongie, and Jan Kautz. Multimodal unsupervised image-to-image translation. In *ECCV*, 2018. 2, 6, 7
- [22] Phillip Isola, Jun-Yan Zhu, Tinghui Zhou, and Alexei A Efros. Image-to-image translation with conditional adversarial networks. In *CVPR*, 2017. 2, 5
- [23] Tero Karras, Samuli Laine, and Timo Aila. A style-based generator architecture for generative adversarial networks. In *CVPR*, 2019. 5
- [24] Junho Kim, Minjae Kim, Hyeonwoo Kang, and Kwanghee Lee. U-gat-it: Unsupervised generative attentional networks with adaptive layer-instance normalization for image-to-image translation. In *ICLR*, 2020. 1, 2, 3, 4, 5, 6
- [25] Jiwon Kim, Jung Kwon Lee, and Kyoung Mu Lee. Accurate image super-resolution using very deep convolutional networks. In *CVPR*, 2016. 1
- [26] Taeksoo Kim, Moon-su Cha, Hyunsoo Kim, Jung Kwon Lee, and Jiwon Kim. Learning to discover cross-domain relations with generative adversarial networks. In *ICML*, 2017. 1, 2
- [27] Diederik P. Kingma and Jimmy Ba. Adam: A method for stochastic optimization. In *ICLR*, 2015. 5
- [28] Pierre-Yves Laffont, Zhile Ren, Xiaofeng Tao, Chao Qian, and James Hays. Transient attributes for high-level understanding and editing of outdoor scenes. *TOG*, 2014. 5
- [29] Xuguang Lai, Xiuxiu Bai, and Yongqiang Hao. Unsupervised generative adversarial networks with cross-model weight transfer mechanism for image-to-image translation. In *ICCV*, 2021. 5, 6
- [30] Hsin-Ying Lee, Hung-Yu Tseng, Jia-Bin Huang, Maneesh Singh, and Ming-Hsuan Yang. Diverse image-to-image translation via disentangled representations. In *ECCV*, 2018. 2, 6
- [31] Hsin-Ying Lee, Hung-Yu Tseng, Qi Mao, Jia-Bin Huang, Yu-Ding Lu, Maneesh Singh, and Ming-Hsuan Yang. Drit++: Diverse image-to-image translation via disentangled representations. *IJCV*, 2020. 6
- [32] Xiaodan Liang, Hao Zhang, and Eric P Xing. Generative semantic manipulation with contrasting gan. In *ECCV*, 2018. 1, 2
- [33] Ming-Yu Liu, Xun Huang, Arun Mallya, Tero Karras, Timo Aila, Jaakko Lehtinen, and Jan Kautz. Few-shot unsupervised image-to-image translation. In *ICCV*, 2019. 2
- [34] Youssef A Mejjati, Christian Richardt, James Tompkin, Darren Cosker, and Kwang In Kim. Unsupervised attention-guided image to image translation. In *NeurIPS*, 2018. 5, 6
- [35] Sangwoo Mo, Minsu Cho, and Jinwoo Shin. Instagan: Instance-aware image-to-image translation. *ICLR*, 2019. 2

- [36] Muhammad Ferjad Naeem, Seong Joon Oh, Youngjung Uh, Yunjey Choi, and Jaejun Yoo. Reliable fidelity and diversity metrics for generative models. In *ICML*, 2020. 5
- [37] Taesung Park, Alexei A Efros, Richard Zhang, and Jun-Yan Zhu. Contrastive learning for unpaired image-to-image translation. In *CVPR*, 2020. 2, 5, 6
- [38] Taesung Park, Ming-Yu Liu, Ting-Chun Wang, and Jun-Yan Zhu. Semantic image synthesis with spatially-adaptive normalization. In *CVPR*, 2019. 2, 5
- [39] Muhammad Usman Rafique, Yu Zhang, Benjamin Brodie, and Nathan Jacobs. Unifying guided and unguided outdoor image synthesis. In *CVPRW*, 2021. 4
- [40] Christos Sakaridis, Dengxin Dai, and Luc Van Gool. Guided curriculum model adaptation and uncertainty-aware evaluation for semantic nighttime image segmentation. In *ICCV*, 2019. 1
- [41] Karen Simonyan and Andrew Zisserman. Very deep convolutional networks for large-scale image recognition. In *ICLR*, 2015. 5
- [42] Hao Tang, Hong Liu, Dan Xu, Philip HS Torr, and Nicu Sebe. Attentiongan: Unpaired image-to-image translation using attention-guided generative adversarial networks. *TNNLS*, 2021. 1, 2, 5, 6
- [43] Hao Tang, Dan Xu, Nicu Sebe, and Yan Yan. Attention-guided generative adversarial networks for unsupervised image-to-image translation. In *IJCNN*, 2019. 2
- [44] Ilya Tolstikhin, Neil Houlsby, Alexander Kolesnikov, Lucas Beyer, Xiaohua Zhai, Thomas Unterthiner, Jessica Yung, Andreas Steiner, Daniel Keysers, Jakob Uszkoreit, et al. Mlp-mixer: An all-mlp architecture for vision. *arXiv*, 2021. 3, 4
- [45] Dmitry Ulyanov, Andrea Vedaldi, and Victor Lempitsky. Instance normalization: The missing ingredient for fast stylization. *arXiv*, 2016. 2, 4
- [46] Ting-Chun Wang, Ming-Yu Liu, Jun-Yan Zhu, Andrew Tao, Jan Kautz, and Bryan Catanzaro. High-resolution image synthesis and semantic manipulation with conditional gans. In *CVPR*, 2018. 2
- [47] Wayne Wu, Kaidi Cao, Cheng Li, Chen Qian, and Chen Change Loy. Transgaga: Geometry-aware unsupervised image-to-image translation. In *CVPR*, 2019. 6
- [48] Shaoan Xie, Mingming Gong, Yanwu Xu, and Kun Zhang. Unaligned image-to-image translation by learning to reweight. In *ICCV*, 2021. 5, 6
- [49] Dan Xu, Wei Wang, Hao Tang, Hong Liu, Nicu Sebe, and Elisa Ricci. Structured attention guided convolutional neural fields for monocular depth estimation. In *CVPR*, 2018. 2
- [50] Chao Yang, Taehwan Kim, Ruizhe Wang, Hao Peng, and C-C Jay Kuo. Show, attend, and translate: Unsupervised image translation with self-regularization and attention. *TIP*. 2
- [51] Guanglei Yang, Hao Tang, Mingli Ding, Nicu Sebe, and Elisa Ricci. Transformer-based attention networks for continuous pixel-wise prediction. In *ICCV*, 2021. 2
- [52] Zili Yi, Hao Zhang, Ping Tan, and Minglun Gong. Dualgan: Unsupervised dual learning for image-to-image translation. In *ICCV*, 2017. 1, 2
- [53] Fisher Yu, Vladlen Koltun, and Thomas Funkhouser. Dilated residual networks. In *CVPR*, 2017. 5
- [54] Richard Zhang, Phillip Isola, and Alexei A Efros. Colorful image colorization. In *ECCV*, 2016. 5
- [55] Richard Zhang, Phillip Isola, Alexei A Efros, Eli Shechtman, and Oliver Wang. The unreasonable effectiveness of deep features as a perceptual metric. In *CVPR*, 2018. 5
- [56] Shengjia Zhao, Jiaming Song, and Stefano Ermon. Infovae: Information maximizing variational autoencoders. *arXiv*, 2017. 4
- [57] Chuanxia Zheng, Tat-Jen Cham, and Jianfei Cai. The spatially-correlative loss for various image translation tasks. In *CVPR*, 2021. 2, 4, 5, 6, 7
- [58] Kaiyang Zhou, Yongxin Yang, Yu Qiao, and Tao Xiang. Domain generalization with mixstyle. *ICLR*, 2021. 4
- [59] Jun-Yan Zhu, Taesung Park, Phillip Isola, and Alexei A Efros. Unpaired image-to-image translation using cycle-consistent adversarial networks. In *ICCV*, 2017. 1, 2, 5, 6
- [60] Jun-Yan Zhu, Richard Zhang, Deepak Pathak, Trevor Darrell, Alexei A Efros, Oliver Wang, and Eli Shechtman. Multi-modal image-to-image translation by enforcing bi-cycle consistency. In *NeurIPS*, 2017. 2
- [61] Peihao Zhu, Rameen Abdal, Yipeng Qin, and Peter Wonka. Sean: Image synthesis with semantic region-adaptive normalization. In *CVPR*, 2020. 2